



POLITECNICO
MILANO 1863

SCUOLA DI INGEGNERIA INDUSTRIALE
E DELL'INFORMAZIONE



One-Dimensional Flow Analysis of a Self-Field Magneto-Plasma Dynamic Thruster

AEROTHERMODYNAMICS PROJECT
SPACE ENGINEERING

Federico Torre, 10645141

Academic year:
2023-2024

Abstract: The paper describes one-dimensional (1D) flow mathematical model to study the physics of fully ionized plasma flow through Magneto Plasma Dynamic Thruster (MPDT). The developed model consists of a set of differential equations obtained by coupling the Navier–Stokes equations with Maxwell’s equations. These simulations have been carried out for a special case of geometries called Tikhonov fitted geometries for alleviating the instability phenomenon commonly known as onset phenomenon in self-field MPDT. All the computations were carried out in Matlab using a higher order integration scheme.

Key-words: MPDTs, computational fluid dynamics, mathematical modeling, Runge - Kutta.

1. Introduction

MPDTs are advanced propulsion devices that generate thrust by ionizing a gas propellant with an electric arc. The ionized plasma is then accelerated by the Lorentz force, which results from the interaction between electric and magnetic fields, producing thrust (see Section 2). In MPDTs, the magnetic field can either be self-induced, as in self-field MPDTs, or externally applied, as in applied-field MPDTs.

The presence of ions, electrons, and neutral particles in the plasma makes its analysis complex. However, under specific conditions, the plasma can be treated as a single conducting fluid using Magneto Hydro Dynamics (MHD) principles. The steady-state, single-fluid model developed in this work aims to explain the acceleration of plasma under the influence of electric and magnetic fields. Despite its simplicity, the model hereafter developed has proven highly effective in illustrating the principles of MPDTs [1].

This work is organized as follows: Section 2 introduces the principles of an MPDT and the assumptions used in the development of the numerical simulation. Section 3 defines the governing equations and provides the matrix form representation useful for the MATLAB code. Subsection 3.1 details the Runge-Kutta method employed, and finally, Section 4 presents the results obtained from the simulation, including a comparison of thruster parameters in cases of constant area, area variation, and heat losses.

2. Theory of MPDT

As defined in 1, MPDTs operate on the principle of electromagnetic acceleration. In its most elementary form, an MPDT consists of a cylindrical cathode surrounded by a concentric anode, as shown in Figure 1. This

involves accelerating a body of ionized gas through the interaction of currents driven through the gas with magnetic fields established either by those currents or by external means.

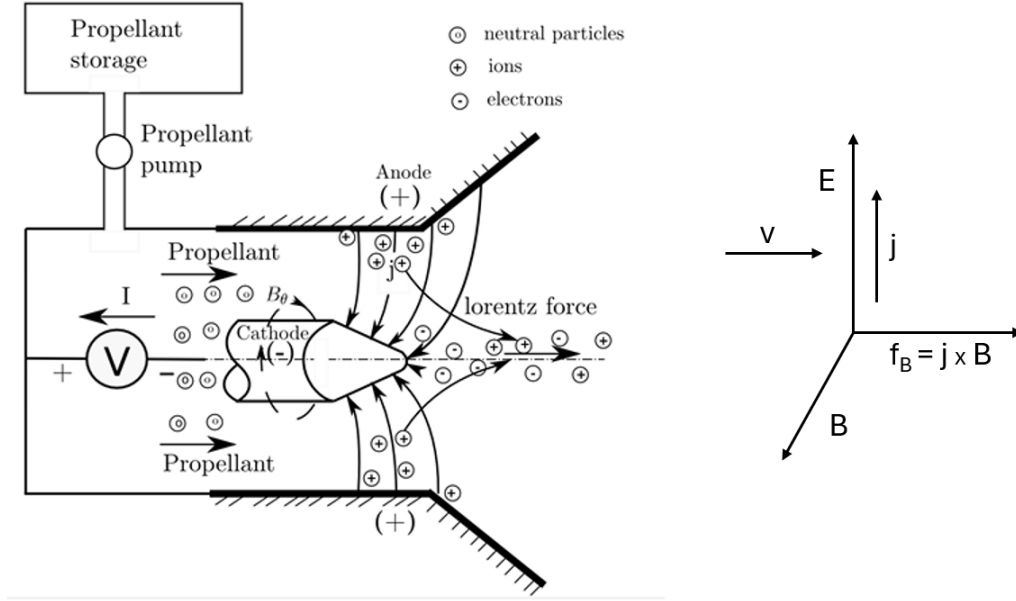


Figure 1: Diagram of an Electric Propulsion (EP) thruster: the MPDT

Consider a flow of ionized gas subjected to an electric field \mathbf{E} and a magnetic field \mathbf{B} , which are perpendicular to each other and to the gas velocity \mathbf{v} . If the gas has a scalar electric conductivity σ , a current density $\mathbf{j} = \sigma(\mathbf{E} - \mathbf{vB})$ will flow through it parallel to \mathbf{E} , and it will interact with the magnetic field \mathbf{B} to provide a distributed body force density $\mathbf{f}_B = \mathbf{j} \times \mathbf{B}$ in the streamwise direction \mathbf{v} , which will accelerate the gas [2].

The main difference between the classic MHD channel analysis and an MPDT analysis is that in the former, the magnetic field is applied with a uniform intensity along the duct. Conversely, in a self-field MPDT, there is only a self-induced magnetic field, which is directly generated by the current flowing between the electrodes and whose intensity is not constant along the channel. Thus, a crucial modification involves removing the assumption of a uniform magnetic field (although \mathbf{E} and \mathbf{B} remain orthogonal). Removing this assumption necessitates the introduction of another equation to describe the evolution of the self-induced magnetic field. For this purpose, the Maxwell Equation (8) that relates the magnetic field to the current density has been introduced in the governing Equations, as seen in Section 2.1.

2.1. Tikhonov Assumptions

Instability phenomenon is common in self-field MPDTs, causing a sudden decrease in the plasma velocity towards the thruster's exit. Tikhonov [5] conducted experiments on both self-field and applied-field MPDT and developed an empirical relation known as Tikhonov's criterion (1). A thruster geometry satisfying this criterion will not suffer from the onset phenomenon and is referred to as a Tikhonov-fitted geometry. Throughout this paper, only Tikhonov-fitted geometries are considered.

$$\frac{r_a}{r_c} > \frac{3.6}{A_o} + 0.5 \quad (1)$$

where r_a, r_c are the radius of the anode and cathode respectively, A_o is a constant obtained from the relation:

$$A_o = \frac{P_{\text{magnetic}}}{P_{\text{gasdynamic}}} = \frac{\gamma}{2} \frac{I^2}{\dot{m}a} \quad (2)$$

where, I is the current density, a is the speed of sound and $P_{\text{magnetic}}, P_{\text{gasdynamic}}$ are the magnetic and gasdynamic pressure, respectively.

Tikhonov proposed a theory based on experiments with various MPDT configurations and developed a 1D MHD model based on the following assumptions:

1. 1D flow
2. $\mathbf{E} \perp \mathbf{B}$
3. $\mathbf{J} \perp \mathbf{B}$

4. Neglect of self-induced magnetic field (only applied field present)
5. Stationary conditions ($\frac{\partial}{\partial t} = 0$)
6. Equal number density and temperature of electrons and ions ($n_e = n_i$, $T_e = T_i$)
7. Constant specific heat ratio ($\gamma = 5/3$, monoatomic gas)
8. The fluid is considered a perfect gas (the equation of state is simply $pv = RT$)

The assumptions above are purely based on 1D MHD flow but in case of MPDT the fourth assumption is not valid and hence only self-induced magnetic field is considered. Based on these assumptions, the governing equations of plasma are:

$$\begin{aligned}
\text{Continuity equation:} \quad & \rho v A = \text{constant}, \\
\text{Momentum equation:} \quad & v \frac{dv}{dz} = -\frac{1}{\rho} \frac{dp}{dz} + \frac{1}{\rho} j B, \\
\text{Energy equation:} \quad & \rho v c_p \frac{dT}{dz} + \rho v^2 \frac{dv}{dz} = j v B + \frac{j^2}{\sigma} (1 - \alpha), \\
\text{Equation of state:} \quad & p = \rho R T, \\
\text{Ohm's law:} \quad & j = \sigma (E - v B), \\
\text{Maxwell equation:} \quad & \frac{dB}{dz} = -\mu_0 j,
\end{aligned} \tag{3}$$

where σ is expressed by the following relation

$$\sigma = \frac{1.5085 \cdot 10^{-2} T^{3/2}}{\ln \lambda}, \quad \text{with: } \ln \lambda \simeq 10.$$

Before proceeding with a numerical solution for this system of differential equations, some notable aspects must be highlighted. By appropriately rearranging the conservation Equations (3), we obtain

$$\frac{dv}{dz} = \frac{1}{(M^2 - 1)} \left[\frac{v}{A} \frac{dA}{dz} - \frac{\gamma - 1}{\rho a^2} \left(\frac{j^2}{\sigma} - Q_{\text{loss}} \right) + \frac{j B v}{\rho a^2} \right] \tag{4}$$

that express the plasma flow acceleration along the channel. Three distinct contributions influence the plasma flow acceleration, and each of them changes sign as the flow transitions from subsonic to supersonic. The first contribution arises from the duct geometry (the flow accelerates in a converging duct when subsonic and in a diverging duct when supersonic). The second one is related to ohmic heating, which significantly accelerates the flow only in the subsonic regime, the last one comes from the Lorentz force, which accelerates the flow in the supersonic regime.

It is evident that at $M = 1$, a singularity occurs because the denominator on the right-hand side goes to zero. This simplified model cannot handle shocks or other discontinuities and fails in the transonic region.

3. Mathematical Model for a Self-field MPD Thruster

An extension of the previous model (3) consists of including the area-variation of the channel. The 1D formulation developed for a self-field MPDT model comprises a set of eight differential equations. These equations were derived from the Navier–Stokes equations, the equation of state, Ohm's law, and Maxwell's equations.

Continuity equation

$$\frac{d\rho}{dz} = -\frac{\rho}{v} \frac{dv}{dz} - \frac{\rho}{A} \frac{dA}{dz} \tag{5}$$

Momentum equation

$$\frac{dv}{dz} = -\frac{1}{\rho v} \frac{dp}{dz} + \frac{j B}{\rho v} \tag{6}$$

Energy equation

$$\frac{dT}{dz} = \frac{j B}{\rho C_p} + \frac{j^2}{\sigma \rho v C_p} (1 - \alpha) - \frac{v}{C_p} \frac{dv}{dz} \tag{7}$$

Maxwell's equation

$$\frac{dB}{dz} = -\mu_0 j \tag{8}$$

Equation of state

$$\frac{dp}{dz} = \rho R \frac{dT}{dz} + R T \frac{d\rho}{dz} \tag{9}$$

Ohm's law

$$\frac{dj}{dz} = \sigma \frac{dE}{dz} - \sigma v \frac{dB}{dz} + B \sigma \frac{dv}{dz} \quad (10)$$

Equation for area variation

$$\frac{dA}{dz} = \frac{2\pi z}{L^2} + \frac{2r_a \tan \theta}{L} \quad (11)$$

Equation for electric field

$$\frac{dE}{dz} = \beta z \quad (12)$$

Where β is the Hall parameter, which is much less than unity for a highly collisional plasma, i.e., $\beta \ll 1$.

To solve the problem the system of equations (5) - (8) is rewritten in the following matrix form

$$A(\mathcal{U}) \frac{d\mathcal{U}}{dz} = \mathbf{F}(\mathcal{U}) \quad (13)$$

where

$$\mathcal{U} = \begin{pmatrix} v \\ \rho \\ T \\ B \end{pmatrix} \quad \mathbf{F} = \begin{pmatrix} f_1(\mathcal{U}, z) \\ f_2(\mathcal{U}, z) \\ f_3(\mathcal{U}, z) \\ f_4(\mathcal{U}, z) \end{pmatrix} \quad A = \begin{pmatrix} 1 & 0 & 0 & 0 \\ \rho/v & 1 & 0 & 0 \\ \rho v^2 & 0 & \rho v C_p & 0 \\ 0 & 0 & 0 & 1 \end{pmatrix}.$$

In order to obtain the normal form of the system (13) is necessary that the matrix A must be invertible, i.e. the determinant $\det(A)$ must be non-zero. In this case, $\det(A) = \rho v C_p \neq 0$, then is possible to rewrite the system as

$$\frac{d\mathcal{U}}{dz} = G(\mathcal{U}) \quad (14)$$

where $G(\mathcal{U}) = A^{-1}F(\mathcal{U})$. The resulting system of equations is given by

$$\begin{cases} \frac{dv}{dz} = f_1(\mathcal{U}, z), \\ \frac{d\rho}{dz} = -\frac{\rho}{v} \cdot f_1(\mathcal{U}, z) + f_2(\mathcal{U}, z), \\ \frac{dT}{dz} = -\frac{v}{C_p} \cdot f_1(\mathcal{U}, z) + \frac{1}{\rho C_p v} \cdot f_3(\mathcal{U}, z), \\ \frac{dB}{dz} = f_4(\mathcal{U}, z). \end{cases} \quad (15)$$

where

$$\begin{aligned} f_1(\mathcal{U}, z) &= \frac{RT v C_p \frac{dA}{dz} - R v j B \rho - \frac{R j^2 (1-\alpha) \rho}{\sigma} + \frac{j B C_p v}{\rho}}{C_p v^2 - R v^2 - C_p R T}, \\ f_2(\mathcal{U}, z) &= -\frac{\rho}{A} \frac{dA}{dz}, \\ f_3(\mathcal{U}, z) &= j v B + \frac{j^2}{\sigma} (1 - \alpha), \\ f_4(\mathcal{U}, z) &= -\mu_0 j. \end{aligned}$$

3.1. Numerical Scheme

The sketch of the numerical scheme, implemented in Matlab, is present in Algorithm 1, it was adapted to integrate a system of first-order differential equations (5) - (12).

Algorithm 1 4th Order Runge-Kutta Method for Solving ODEs

```

1: Input: odefun (Function handle for the ODE system),  $y_0$  (Initial state variables vector),  $h$  (Step
   size for the integration).
2: Output:  $z$  (Vector of  $z$  positions),  $Y$  (Matrix of state variables at each  $z$  position)
3: Initialize arrays:
4:  $Y \leftarrow \text{zeros}(\text{length}(y_0), nsteps + 1)$ 
5:  $Y(:, 1) \leftarrow y_0$ 
6: for  $k \leftarrow 1$  to  $nsteps$  do
7:    $k1 \leftarrow h \cdot \text{odefun}(z(k), Y(:, k), params)$ 
8:    $k2 \leftarrow h \cdot \text{odefun}(z(k) + \frac{h}{2}, Y(:, k) + \frac{k1}{2}, params)$ 
9:    $k3 \leftarrow h \cdot \text{odefun}(z(k) + \frac{h}{2}, Y(:, k) + \frac{k2}{2}, params)$ 
10:   $k4 \leftarrow h \cdot \text{odefun}(z(k) + h, Y(:, k) + k3, params)$ 
11:   $Y(:, k + 1) \leftarrow Y(:, k) + \frac{1}{6}(k1 + 2k2 + 2k3 + k4)$ 
12: end for

```

4. Results of Numerical Simulations

The self-field MPDT simulation uses Tikhonov-fitted geometries (see Section 2.1). These geometries are designed to remain stable throughout the flow. The objective of developing this model and conducting numerical simulations is to demonstrate that if a particular MPDT configuration satisfies Tikhonov's criterion, it will avoid the instability problems inherent in MPDTs and maintain acceleration throughout the channel. The code is structured to verify whether a chosen geometry adheres to the constraint defined in Equation (1).

4.1. Initial Conditions

The initial conditions for the self-field MPDT simulation, listed in Table 1, were derived from fundamental relations such as the equation of state, Mach number, and the Spitzer-Härm relation [4].

Initial & Operating Conditions		Duct Geometry	
Density	$5.88701964 \times 10^{-6} \text{ kg/m}^3$	Anode radius	0.126 [m]
Pressure	14.218 Pa	Cathode radius	0.036 [m]
Velocity	2207.139 m/s		
Area	0.05 m ²		
Magnetic Field	0.001 T		
Electric Field	39.325 V/m		
Temperature	11605.0 K		
Current Density	3500.0 A/m ²		

Table 1: Initial and operating conditions alongside duct geometry.

4.2. Validation of the Code

The model was tested with a duct length of 7 cm, and the results do not account for heat losses ($\alpha = 0$). The code developed here has been validated against the work by Mariano Andrenucci from the University of Pisa [6]. Figure 2 shows the two models considered. In Section 3, the system of equations accounts for area variation, whereas in [6], a constant area is assumed. When the area variation is set to zero in (5) - (12), the results are in agreement with those developed by the University of Pisa. Figure 2 demonstrates that the variables follow the same trend, confirming the accurate reproducibility of the code.

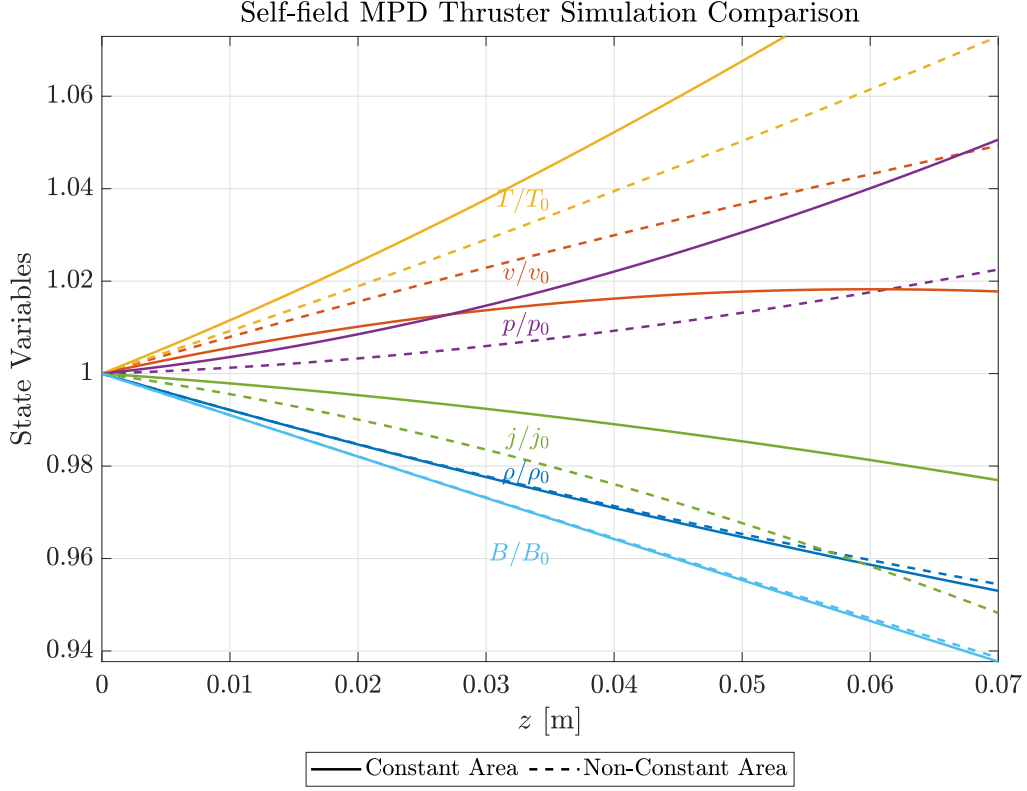


Figure 2: 1D Flow Simulation.

To assess the effect of varying the cross-sectional area along the channel, a slightly divergent duct is investigated. The aperture angle θ must be small; otherwise, the assumption of 1D flow would no longer be valid. With a slightly diverging duct, a higher exhaust velocity is obtained (Figure 3) due to the gas-dynamic contribution [1, 5, 6]. A greater electrode distance at the end of the channel leads to a reduction in the electric field intensity, causing the current density to assume lower values compared to the case of a constant area. A duct shape that follows the current density distribution was previously proposed by Kuriki [6], aiming for a narrower channel where j is lower and a wider channel where j is higher.

According to Ohm's law, Eq.(10), the current density is actually higher near the inlet, where the flow velocity is lower. The flow velocity increases consistently along the channel, except near the exit section. This anomaly is due to a rapid pressure rise, which is an immediate consequence of the temperature increase.

An important observation from Figure 3 is that the magnetic field decreases as the flow moves away from the inlet.

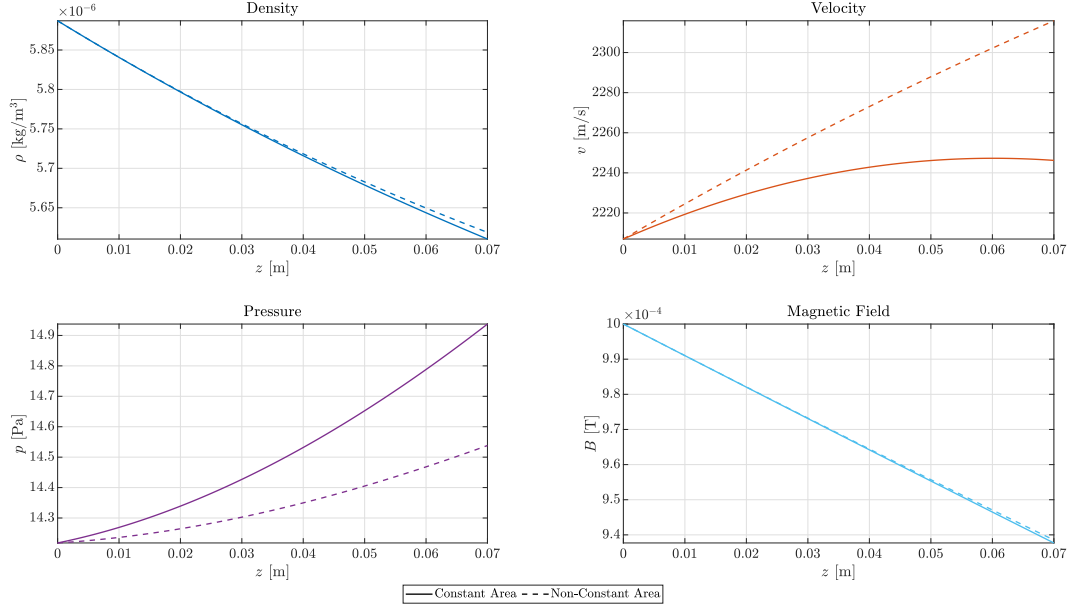


Figure 3: Behavior of the thruster parameters.

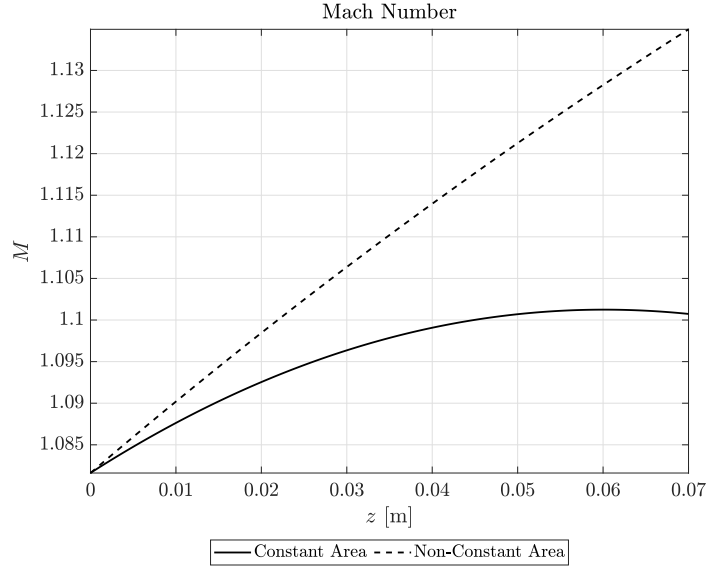


Figure 4: Mach number evolution.

Figure 4 shows that, to avoid singularity at $M = 1$, a fully supersonic flow has been analyzed (see Section 2.1). In a real MPDT, the flow is expected to rapidly become supersonic and then be further accelerated by the Lorentz force along the rest of the channel. Thus, assuming a fully ionized flow with an initial Mach number slightly greater than one is a reasonable choice [6].

4.3. Effect of Heat Losses

Assuming a non-zero value for α implies that a portion of the heat generated by the current is dissipated to the walls. To illustrate the effect of heat losses, a simulation was conducted with non-zero value of the parameter α , for example $\alpha = 0.3$ as in [6]. The results of this simulation are presented in Figure 5. In which is possible to observe that the removal of heat from the flow results in a temperature decrease, which in turn, leads to a pressure decrease. Additionally, the figure indicates that lower pressure leads to an increase of velocity. It is also important to note that a longer channel is required to sustain the current when there is heat loss. This

is because lower thermal conductivity, associated with heat losses, results in a lower temperature, necessitating an extended channel length to maintain the desired flow parameters.

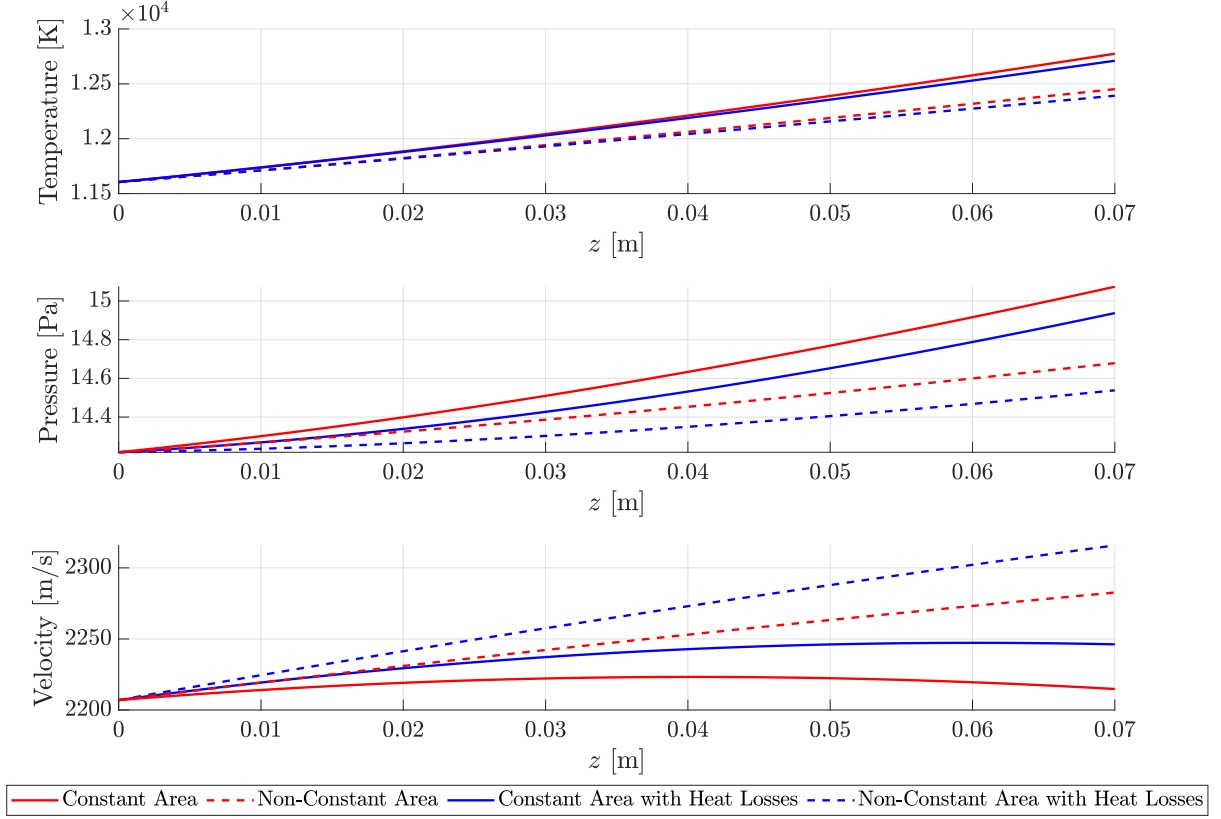


Figure 5: Effect of heat losses ($\alpha = 0.3$) on the thruster parameters: Temperature, Pressure and Velocity profiles.

5. Conclusion and Future Work

A 1D model has been developed to investigate a self-field MPDT. The model is based on the assumptions of MHD and Tikhonov's criterion. Several numerical simulations have been conducted to highlight various aspects of the plasma acceleration process. The effect of a variable cross-section has been examined, resulting in a higher exhaust velocity due to the gas-dynamic component of the acceleration, as well as lower temperatures and current densities. Additionally, the impact of heat losses along the channel has been studied, revealing a reduction in temperature [6].

The methodology presented provides a useful framework for understanding the physics behind an MPDT; however, it should not be considered a definitive reference for design purposes. One of the primary limitations is that the model fails to accurately capture electromagnetic interactions. For instance, when pressure decreases, the continuum flow approximation becomes invalid, and the Maxwellian assumption no longer holds (see Section 2.1).

Simulating plasmas for applications such as space electric propulsion is inherently complex due to two key factors. First, the system size of interest is often comparable to the collisional length scale because of the low pressure, leading to velocity distributions that are not always in equilibrium. Second, the length and time scales of interest are typically much larger than the natural length and time scales of the plasma, which are dictated by the fast-moving electrons. This can make simulations extremely computationally expensive. Employing particle methods, particularly the hybrid Particle-in-Cell-Direct Simulation Monte Carlo (PIC-DSMC) method, offers an efficient approach to addressing the first challenge, as phase space can be represented using computational particles [3].

Nomenclature

Variable	Description
B	Magnetic Field
j	Current Density
R	Gas constant
M	Mach number
γ	Specific heat ratio
a	Sound speed
θ	Angle of inclination with respect to z
μ_0	Vacuum magnetic permeability
σ	Electric conductivity
λ	Plasma parameter
β	Hall parameter
c_p	Specific heat at constant pressure
A_0	Tikhonov's Criterion Constant
r_a	Anode Radius
r_c	Cathode Radius
\dot{m}	Mass flow rate of gas
L	Length of the channel
$P_{\text{gasdynamic}}$	Gas dynamic pressure
P_{magnetic}	Magnetic pressure
ρ	Plasma density
A	Channel cross-sectional area
v	Velocity
z	Spatial coordinate
α	Fraction of Joule heating going into heat losses
p	Pressure
T	Temperature
Q_{loss}	Heat loss

References

- [1] Raman Balu and Vijai Kumar. Numerical simulation of magnetohydrodynamic flow through a magneto-plasma dynamic thruster. In *Proceedings of the Modeling, Simulation, and Scientific Computing Conference*, 2013.
- [2] Charles Chelem Mayigué. *Numerical investigation of MPD thrusters using a density-based method with semi-discrete central-upwind schemes for MHD equations*. PhD thesis, UNIVERSITÄT BREMEN, 2018.
- [3] Pietro Parodi, Giovanni Lapenta, and Thierry Magin. Simulation of plasmas for electric propulsion using the energy-conserving semi-implicit pic scheme. In *Proceedings of the 9th European Conference for Aeronautics and Space Sciences (EUCASS)*, 2022.
- [4] L. Spitzer and R. Harm. Transport phenomena in a completely ionized gas. *American Physical Society*, 89:977–981, 1953.
- [5] Thanigaiarasu Subramanian. A new mathematical model for studying fully ionized plasma flows in mpd thrusters. *Modeling Simulation and Scientific Computing*, 2016.
- [6] Mariano Andrenucci Tommaso Misuri. Mhd plasma flows in a 1d channel. *Congresso Nazionale AIDAA*, 2009.